Daniele Borzelli et al 2020 J. Neural Eng. 17 016058
Doi: 10.1088/1741-2552/ab6d88
https://iopscience.iop.org/article/10.1088/1741-2552/ab6d88

Identification of the best strategy to command variable stiffness using electromyographic signals

Daniele Borzelli[1,2], Etienne Burdet[3], Stefano Pastorelli[2], Andrea d'Avella[1,4], Laura Gastaldi[5]

E-mail: dborzelli@unime.it

[1]Department of Biomedical and Dental Sciences and Morphofunctional Imaging, University of Messina, Italy
[2]Department of Mechanical and Aerospace Engineering, Politecnico di Torino, Turin, Italy
[3]Department of Bioengineering, Imperial College of Science, Technology and Medicine, London, United Kingdom
[4]Laboratory of Neuromotor Physiology, IRCCS Santa Lucia Foundation, Rome, Italy
[5]Department of Mathematical Sciences, Politecnico di Torino, Turin, Italy

ORCID:
Daniele Borzelli: 0000-0002-9456-0177
Etienne Burdet: 0000-0002-2123-0185
Stefano Pastorelli: 0000-0001-7808-8776
Andrea d'Avella: 0000-0002-3393-4956
Laura Gastaldi: 0000-0003-3921-3022

Keywords:
Impedance control, EMG-driven, robotic device, exoskeleton, motor control, wrist, Hi-5

Abstract

Objective. In the last decades, many EMG-controlled robotic devices were developed. Since stiffness control may be required to perform skillful interactions, different groups developed devices whose stiffness is real-time controlled based on EMG signal samples collected from the operator. However, this control strategy may be fatiguing. In this study, we proposed and experimentally validated a novel stiffness control strategy, based on the average muscle co-contraction estimated from EMG samples collected in the previous 1 or 2 seconds. *Approach*. Nine subjects performed a tracking task with their right wrist in five different sessions. In four sessions a haptic device (Hi-5) applied a sinusoidal perturbing torque. In Baseline session, co-contraction reduced the effect of the perturbation only by stiffening the wrist. In contrast, during aided sessions the perturbation amplitude was also reduced (mimicking the effect of additional stiffening provided by EMG-driven robotic device) either proportionally to the co-contraction exerted by the subject sample-by-sample (Proportional), or according to the average co-contraction exerted in the previous 1s (Integral 1s), or 2s (Integral 2s). Task error, metabolic cost during the tracking task, perceived fatigue, and the median EMG frequency calculated during a sub-maximal isometric torque generation tasks that alternated with the tracking were compared across sessions. *Main results.* Positive effects of the reduction of the perturbation provided by co-contraction estimation was identified in all the investigated variables. Integral 1s session showed lower metabolic cost with respect to the Proportional session, and lower perceived fatigue with respect to both the Proportional and the Integral 2s sessions. *Significance.* This study's results showed that controlling the stiffness of an EMG-driven robotic device proportionally

to the operator's co-contraction, averaged in the previous 1s, represents the best control strategy because it required less metabolic cost and led to a lower perceived fatigue.

1. Introduction

The use of electromyographic (EMG) signals to control robotic systems [1], in particular limb prostheses [2] and exoskeletons [3], is a long standing idea. Since the EMG signal is occurring 30-100 ms before the development of muscle tension, the motor command can be identified ahead of the movement thus potentially enabling a smooth and intuitive control of the robotic device without delay and without resistance in the case of an exoskeleton [3]. Therefore, many robotic devices have implemented force generated as a function of the operator muscles' EMG [4]–[9]. Furthermore, skillful interaction control may require stiffness control [10]. Therefore, several groups have implemented real-time EMG based stiffness control of robotic devices [11]–[18]. However, in these previous studies, the robot's stiffness was computed sample-by-sample from the operator's EMG signal, a strategy that may not be optimal for the operator. In fact, subjects using such command strategy were observed to yield high stiffening [19] which may be very tiring. A command strategy that keeps the stiffness generated by the robot at a level that corresponds to the previous stiffness (i.e. the co-contraction) generated by the operator may be more appropriate.

We therefore decided to test different command strategies for a robot's stiffness control. In five sessions performed on different days, participants were asked to flex and extend their right wrist for tracking a virtual cursor while a haptic device applied a torque perturbation. During three out of five sessions (so-called "aided sessions"), the amplitude of the perturbation was reduced proportionally to the co-contraction of two antagonist wrist muscles (the Flexor Carpi Radialis and the Extensor Carpi Radialis). The reduction was performed in three different ways: the amplitude of the perturbation was reduced by the sample-by-sample co-contraction (Proportional sessions), by the mean co-contraction exerted during the previous 1 s (Integral 1s), or by the mean co-contraction exerted during the previous 2 s (Integral 2s). The effects of these three command strategies were investigated in terms of muscle fatigue, task error, energy consumption, and perceived fatigue. They were then compared with two other sessions, in which no reduction of the perturbation was provided (Baseline session) and in which no perturbative torque occurred (Control session).

If subjects maintained a constant level of co-contraction, the three aided sessions would be indistinguishable in terms of performance, fatigue and metabolic cost. On the contrary, the Integral control strategies would allow the Central Nervous System to exploit different strategies that would generate the same tracking error with lower metabolic cost, e.g. increasing the co-contraction level during those phases in which the activation required to move the wrist was lower and reducing it when the activation required to move the wrist was higher. Since we expected that the Central Nervous System would exploit a less energy consuming solution, we hypothesize that an Integral control strategy would be preferable respect with the Proportional one.

2. Methods

Daniele Borzelli et al 2020 J. Neural Eng. 17 016058
Doi: 10.1088/1741-2552/ab6d88
https://iopscience.iop.org/article/10.1088/1741-2552/ab6d88

2.1. Participants

The study was approved by the ethical committee of Imperial College London and all participants gave their informed consent prior to participation. Nine right-handed participants, aged between 24 and 34 (mean ± std: 27.7 ± 4.0, 4 females), participated in the experiment. All participants were naïve to the experimental conditions and had no known neuromuscular disorder or recent injury on the right wrist.

2.2. Setup

Experiments were conducted using the Hi5 robotic interface [20]. This is a wrist interface fixed to a table on which the participant places the (right) arm, holds the handle, and interacts with wrist flexion/extension movements (Fig. 1A). The Hi5 is equipped with a DC motor (MSS8, Mavilor) which allows to program the torque exerted on the wrist joint, and a 5000 cycles per revolution differential encoder (RI 58-O, Hengstler) to measure the wrist angle. A torque sensor (TRT-100, Transducer Technologies) is also mounted between the rotating shaft and the handle of the device. Two steel bars, limiting the motion range for safety, are adjusted to each participant (Fig. 1B-C). The device is controlled via Labview Real-time v11.0 using a dedicated target PC computer running on a Real-Time OS that reads the sensor inputs, processes them, and sets the outputs (motor command to the servo amplifier) at 1kHz through a data acquisition card (DAQ-PCI-6221, National Instruments). Visual feedback of the participant's wrist angle and exerted torque is provided on a monitor placed in front of the participant (Fig. 1D). The wrist angular position and torque are recorded at 100 Hz.

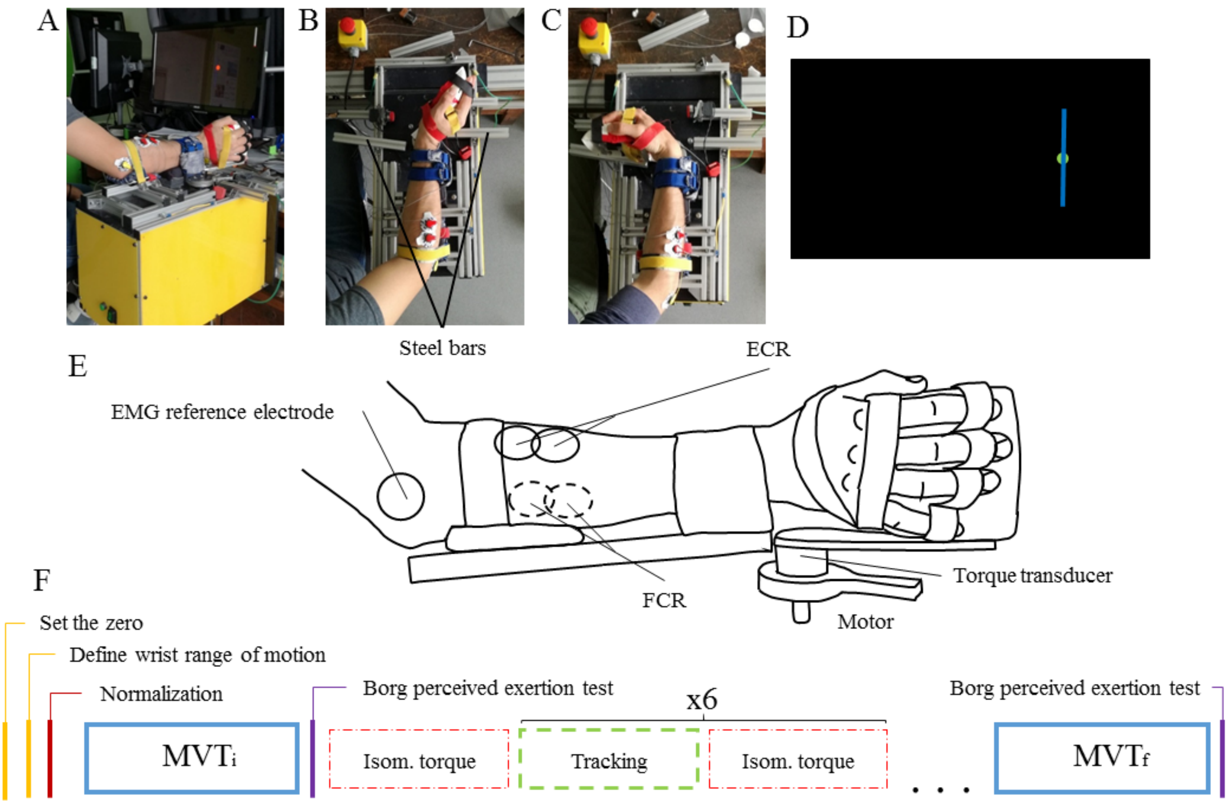

Fig. 1: Setup and protocol. A-C. The Hi5 robotic wrist flexion/extension interface (A), with the wrist completely extended (B) and participant completely flexed (C). The steel bars against which the participant

exerted the isometric force are indicated. (D) Visual display to the participant. The circle is the target of force or position that the participant had to reach. The circle was red if the participant was outside it, or green if the participant was within the boundaries. The blue bar displacement was proportional to the participant's wrist position or to the torque the participant was exerting with their wrist. (E) Schematic of the setup in which the torque transducer, the motor, and the EMG positioning are indicated. (F) Experimental protocol. After the identification of the zero/rest position and the wrist range of motion, the maximum co-contraction was measured and used to normalize the EMG signals. Then the maximum voluntary torques (MVT_i) in the flexion and extension directions were recorded and used to normalize the torque. Seven isometric tasks, in which the participant was asked to reach a torque target, alternated with six tracking tasks, in which the participant was asked to move their wrist to track a virtual cursor while an external perturbation was applied. The perturbation level did depend on the session. Finally, the participant was asked to exert the maximum voluntary torques (MVT_f) again at the end of the session.

Surface EMG signals of the Flexor Carpi Radialis (FCR) and the Extensor Carpi Radialis longus (ECR) muscles, which are prime movers of the wrist flexion and extension in a midway position [21], were recorded (Fig. 1E). The electrode position was determined for each muscle based on the location suggested by the SENIAM project [22] and using functional maneuvers [23]. The area was cleansed with alcohol. Disposable pre-gelled adhesive electrodes (Kendall/Tyco H135SG) were fixed to the participant's skin (inter-electrode distance: ~1cm) and a ground electrode was fixed on the participant's lateral epicondyle. The EMG signals were pre-amplified using active clip connectors (g.GAMMAclip + g.GAMMABox, g.Tec, Austria) and amplified using a medically-certified amplifier (g.BSamp, g.Tec, Austria). Data were then collected at 1000 Hz using a A/D data acquisition card (NI 6221, National Instruments). EMG data were processed offline for subsequent analysis. A zero-lag fourth-order 20–500 Hz band-pass Butterworth filter was first used to filter out cable movements' artifacts and high frequency noise components. The signal was then rectified and low-pass filtered using a zero-lag fourth order Butterworth filter with 5 Hz cut-off frequency and resampled at 100 Hz. Data analysis was performed using custom made Matlab software and statistics with GraphPad Prism 5.

2.3. Protocol

Each participant performed five experimental sessions on five different days. The experimental protocol, illustrated in Fig.1(F), includes the following procedures:

Setting of the zero, definition of the wrist range of motion and normalization. Participants' forearm and hand were fixed to the Hi5 device. At the beginning of each session, participants were asked to place their wrist in the most comfortable position and to relax their muscles. This "rest position" was set as the reference position, relative to which participants were then asked to maximally flex and extend their wrist to reach the maximum angles they felt comfortable. Two steel bars were set at these maximum comfortable flexion ($angle_F$, positive) and extension ($angle_E$, negative) angles (Fig. 1(B-C)). Then the mean rest value was estimated when the participant was relaxing his/her forearm, as well as the mean maximum co- contraction, estimated when the participant maximally co-contracted his/her wrist such to keep a virtual cursor within a target positioned at 0° for 4s when a perturbation (3 Hz sinusoidal trajectory of 10° amplitude, 0°- centered) was applied [21].

The EMG data of both FCR and ECR were normalized with respect to the mean maximum co-contraction and the mean rest value was subtracted. Since a unique normalization across subjects may hide the principal differences across different sessions, because weaker subjects may perceive all the sessions too hard and stronger subjects may perceive all the sessions too easy to be performed, a subject-specific normalization was used. Wrist extension and the corresponding torque that made the wrist to extend was considered as positive, while wrist flexions and the corresponding torques that made the wrist to flex were negative.

Initial Maximum Voluntary Torques (MVT$_i$) exertion and Borg scale administration. Participants were asked to flex their wrist until it reached the steel bar placed at $angle_F$ and to exert the maximum torque against it until the monitor scene changed (MVT_{Fi} block). The whole flexion block lasted 10 s. Participants were then asked to relax for 5 s and to extend their wrist until it reached the steel bar placed at $angle_E$ and to exert the maximum torque against it until the monitor scene changed (MVT_{Ei} block). The whole extension block also lasted 10 s. After 5 s of relaxation both MVT blocks were repeated a second time. During all the repetitions participants were encouraged to exert their maximum torque with verbal encouragements like “go”, or ”more” [24]. The MVT_{Fi} (MVT_{Ei}) was defined as the negative (positive) peak of torque calculated during the two repetitions of the MVT_{Fi} (MVT_{Ei}) block, respectively. The Borg RPE CR10 scale [25] was used to identify the participant perceived exertion.

Isometric task. During the next block (Isometric torque block), visual feedback of the exerted isometric torque was provided to the participant as the displacement of a blue cursor bar (Fig. 2, upper panel). The block was composed of two trials: the first required the generation of an isometric flexion torque and the second the generation of an isometric extension torque. During the generation of the isometric flexion (extension) torque a circular target was displayed in a position that corresponded to 20% MVT_{Fi} (MVT_{Ei}), with a radius of 2% MVT_{Fi} (MVT_{Ei}) (red/green circle in Fig. 2). Therefore, the participant was asked to flex (extend) their wrist and exert a force against the steel bar, such as to move the cursor inside the target and keep it within for 2 s. The target color was red when the cursor was outside the target (i.e. the participant did not match the isometric torque target) and green when the cursor was inside the target (i.e. the participant exerted a torque within the target boundaries). The isometric task was repeated 7 times, alternated with a tracking task (see below), and it allowed to calculate the time-course of fatigue, measured as the median frequency of the EMG signal collected from the ECR and the FCR, during the experiment.

Daniele Borzelli et al 2020 J. Neural Eng. 17 016058
Doi: 10.1088/1741-2552/ab6d88
https://iopscience.iop.org/article/10.1088/1741-2552/ab6d88

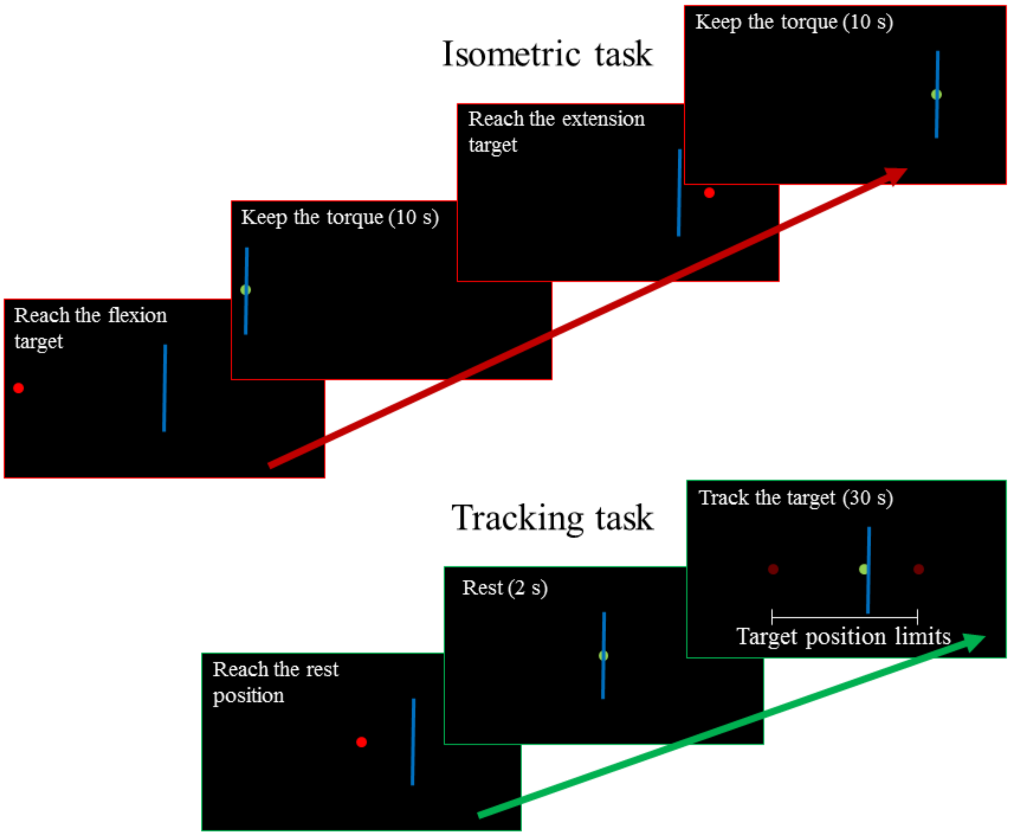

Fig. 2: Isometric (upper) and tracking (lower) tasks.

Tracking task. After 2 s rest, participants were asked to flex/extend their wrist for 30 s in order to track the circular target. Participants received feedback of the wrist angle as the displacement of a blue cursor bar (Fig. 2, lower panel). The spherical target had a radius corresponding to 2% of the minimum between $angle_F$ and $angle_E$ and moved with a sinusoidal motion whose amplitude was 80% of the minimum between $angle_F$ and $angle_E$. The amplitude of the first half of the sinusoid grew with time to permit participants to better adapt to the task. The target frequency was set such that in 30 s the target made 7 complete sinusoids (frequency 0.23 Hz). This frequency allowed participants to easily track the target. The target became red if the cursor was outside the target and green if it was inside it.

During the tracking, the test bench motors applied a 3 Hz sinusoidal torque perturbation at the wrist with a varying amplitude, depending on the implemented command strategy as described below. During the task, if the experimenter noticed a performance reduction, vocal gratifications and encouragement (e.g. “try to do better”, “you are going well”, “you are improving your performance”) were given to the participant such as to help them focusing on the task. The tracking task was repeated six times, alternated with the isometric task (see above Fig. 1(F)).

Command strategies. The participant could reduce the effect of the torque perturbation in different ways, depending on the specific strategy implemented in each session:

- *Baseline session*: the torque perturbation amplitude was set to 10% of the mean absolute value between MVT_{Fi} and MVT_{Ei}. During this session, participants could reject the perturbation by stiffening their wrist.

Doi: 10.1088/1741-2552/ab6d88
https://iopscience.iop.org/article/10.1088/1741-2552/ab6d88

- *Proportional session*: the torque perturbation amplitude was set to 10% of the mean absolute value between MVT_{Fi} and MVT_{Ei}. However, the amplitude of the perturbation was reduced proportionally to the sample-by-sample co-contraction (see Fig. 3). Co-contraction was defined as the minimum between the FCR and ECR sEMG signals, normalized to the maximum voluntary co-contraction. The perturbation amplitude assumed its maximum value if no co-contraction was detected and it was = 0 if the co-contraction was >= 0.25. This command strategy was inspired by the command implemented in exoskeletons to enhance the operator's force based on the EMG signal [3], [13].
- *Integral 1s session*: similar to the proportional session, but with the perturbation amplitude reduced proportionally to the mean co-contraction exerted by the participant 1 s before the current time.
- *Integral 2s session*: similar to the Integral 1s session with perturbation amplitude reduced proportionally to the mean co-contraction exerted 2 s before the current time.
- *Control session*: no perturbation was applied to the participant during the tracking.

The Baseline session was performed on the first day, the aided sessions (Proportional, Integral 1s and Integral 2s) were randomly shuffled for each participant and were performed during the second, third and fourth days, and the Control session was performed on the fifth day. The aided sessions were simulating the aid performed by an external device and the threshold level of 0.25 of co-contraction identified the level over which the device exerts its maximum aid. Since the purpose of the simulated external device was to avoid fatigue in the operator, the value of 0.25 was defined because it was a non-fatiguing contraction. In fact, the complete pool of the motor units of one muscle was commonly recruited for activations higher than 0.5 of the maximum voluntary contraction, as showed in the literature [26].

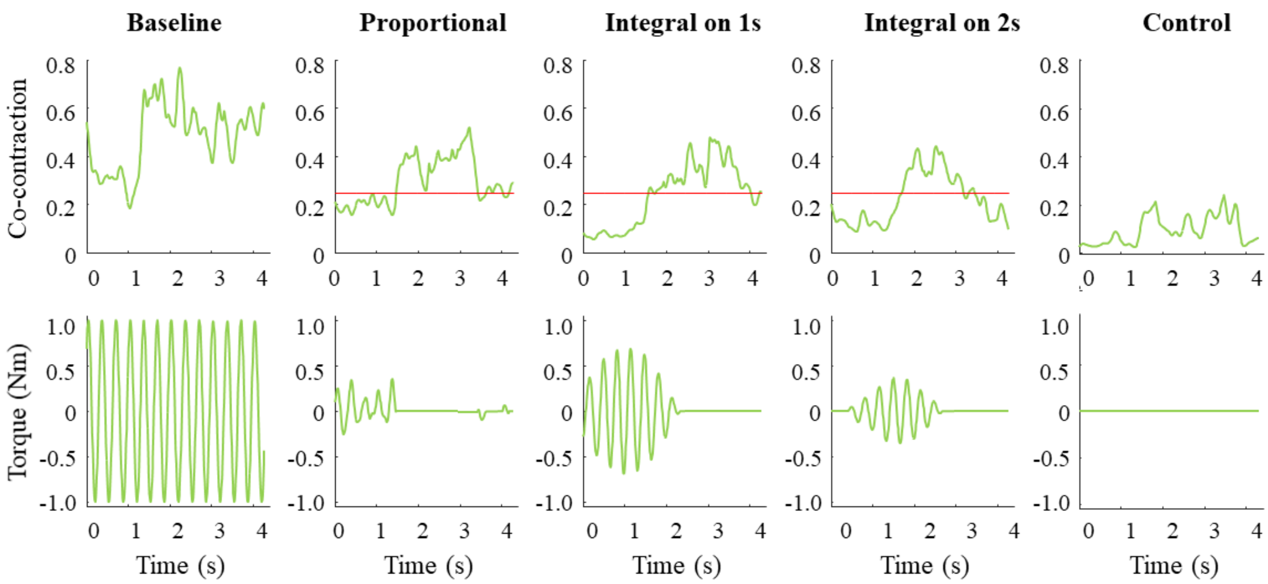

Fig. 3: Co-contraction (upper figures) and torques (lower figures) exerted during a time interval in which the target moves along a complete sinusoid. The red lines in the co-contraction panels of the aided sessions indicate the 0.25 threshold above which no torque perturbation is delivered.

Final Maximum Voluntary Torques (MVT_f) exertion and Borg scale administration. After the last isometric task, repetition the participant was asked to exert again the maximum voluntary torque of flexion (MVT_{Ef}), and extension (MVT_{Ff}) as previously described for the calculation of MVT_{Fi} and MVT_{Ei}. At the very end of the experiment, the rating of perceived exertion, based on the Borg RPE CR10 scale, was communicated by the participant.

2.4. Task error during tracking

The task error e that participants committed during the tracking task was calculated for each session and subject as

$$e = \sqrt{\frac{\sum_{i=1}^{n_{samples}} \left(w_{a_i} - t_{a_i}\right)^2}{n_{samples}}}$$

with w_a the wrist angle, t_a the target angle, $n_{samples}$ the number of samples acquired during each repetition. Since a decrease in the task error was observed between the first and the other repetitions of the baseline session (see Fig. 4), probably due to the familiarization with the task, the first repetition of each session was excluded from the statistical analysis.

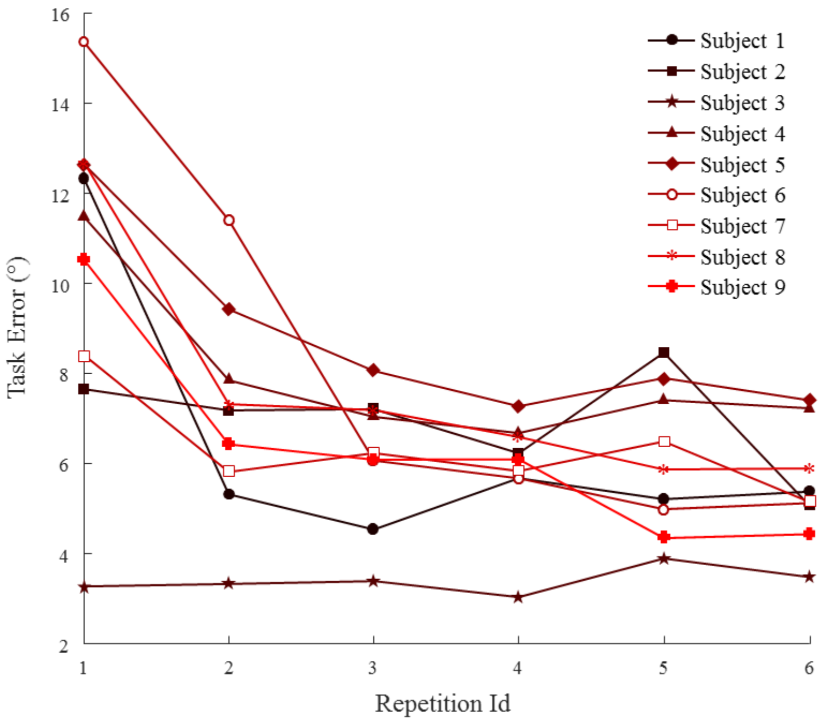

Fig. 4: Task error committed by each participant during all the repetition of the Baseline session. A consistent decrease was observed between the first and the second repetitions.

2.5. Metabolic cost during tracking

The metabolic cost ε was calculated during the tracking task of all the sessions as

$$\varepsilon = \sum_{i=1}^{n_{samples}} (m_{ECR}^2 + m_{FCR}^2)$$

where m_{ECR} and m_{FCR} were the recorded activations of the ECR and the FCR respectively. Raw EMG data, second order Butterworth band-pass filtered between 20 and 500 Hz were used. The energy consumption was evaluated for each participant, session, and repetition. Consistently with the analysis performed on task error, the first repetition of all the sessions was excluded from the statistical analysis of the energy consumption.

2.6. Perceived fatigue

The overall perceived fatigue was expressed by the participant based on the Borg RPE CR10 scale, which was filled at the beginning (PF_i) and at the end (PF_f) of each session. The PF_i was measured to identify if there was a bias in the perceived fatigue, while the PF_f to compare the perceived fatigue across sessions.

2.7. Median EMG frequency during the isometric task

The raw EMGs, recorded at 1000 Hz during all the repetitions of the isometric flexion and extension tasks, were Butterworth second order filtered between 20 and 500 Hz to calculate the Welch's power spectral density $PS(f)$ [27] and to estimate muscular fatigue. The Welch's power spectral density, which is a function of the frequency f, was calculated for each repetition of both the flexion and extension tasks, with a number of overlapping points equal to 500 (0.5 s), with the Matlab function 'pwelch'. To examine fatigue, we considered the median frequency F_{median} that separates the EMG power spectrum into two parts of equal energy [28]:

$$\int_{f_1}^{F_{median}} PS(f) \cdot df = \int_{F_{median}}^{f_2} PS(f) \cdot df$$

where f_1=20Hz and f_2=500Hz define the bandwidth of the sEMG signal. The ECR and FCR median frequencies were calculated during each repetition of each session of both flexion and extension isometric tasks. The increase of the median frequency indicated the occurrence of fatigue and the regression of the median frequency [26] on the repetition was calculated from the FCR, during the isometric flexion task, and from the ECR, during the extension task, for each participant and each session.

2.8. Statistics

The Friedman test for paired non-parametric data was performed to identify significant differences between the perceived fatigues at the beginning and end of the different sessions, and a Wilcoxon signed-rank test was used as post-hoc test to identify differences among perceived fatigue in pairs of sessions. One-way repeated measures ANOVA was performed to identify significant differences between the MVT_{Fi} and the MVT_{Ei}, and the slopes of the median frequency, across different repetitions. Two-way repeated measurements ANOVA was performed to identify significant differences among the task error and the metabolic cost calculated during different sessions and repetitions. Paired t-test was implemented as post-hoc test to identify differences among data collected during pairs of sessions. The GraphPad Prism 5 software was used to perform statistical analysis.

3. Results

During the tracking task, the participants were able to both track the cursor and to increase the co-contraction level such as to reduce the torque perturbation. Therefore, they were able to coordinate muscles such as to simultaneously track the target and modulate stiffness (see Fig. 5).

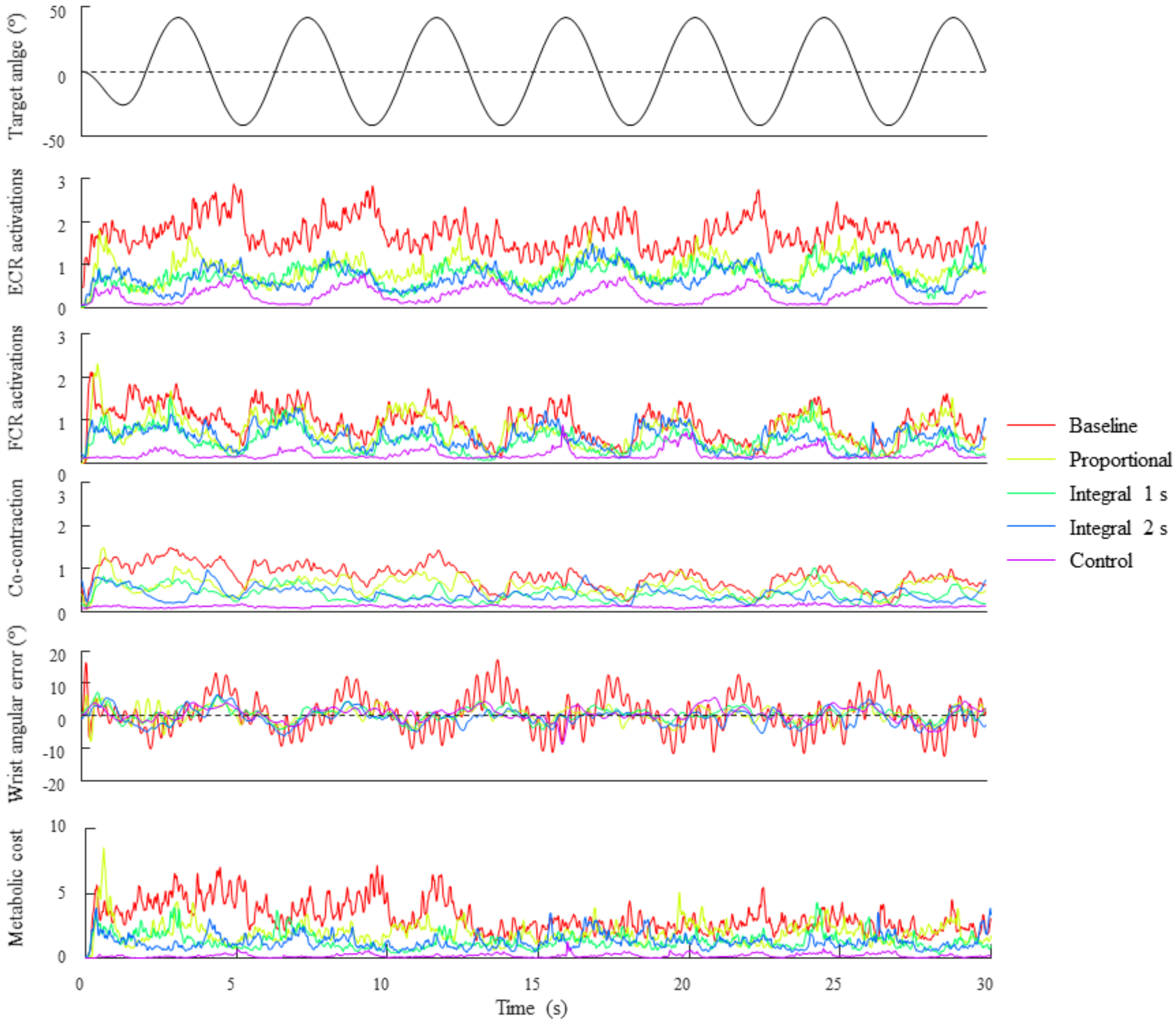

Fig. 5: Example of one repetition of the tracking task. Target angle, ECR and FCR activations (Butterworth 2nd order filtered between 20 and 500 Hz, rectified, resampled at 100 Hz, baseline subtracted and normalized, and averaged across the repetitions of the dynamic task), co-contraction, wrist angular error (intended as the difference between the participant's wrist angle and the target angle, averaged across the repetitions of the dynamic task), and metabolic cost (intended as the square sum of the ECR and FCR) recorded from participant 1 are shown. Different colors correspond to different sessions.

The simultaneous activation of ECR and FCR muscles were not ascribed to pick-up of the signal from one muscle by the electrode on the other muscle (cross-talk). In fact, during the tasks in which no co-contraction was required (i.e the MVT and the isometric tasks) a clear distinction between the activations of the agonist and the antagonist muscles was observed (e.g. see Fig. 6).

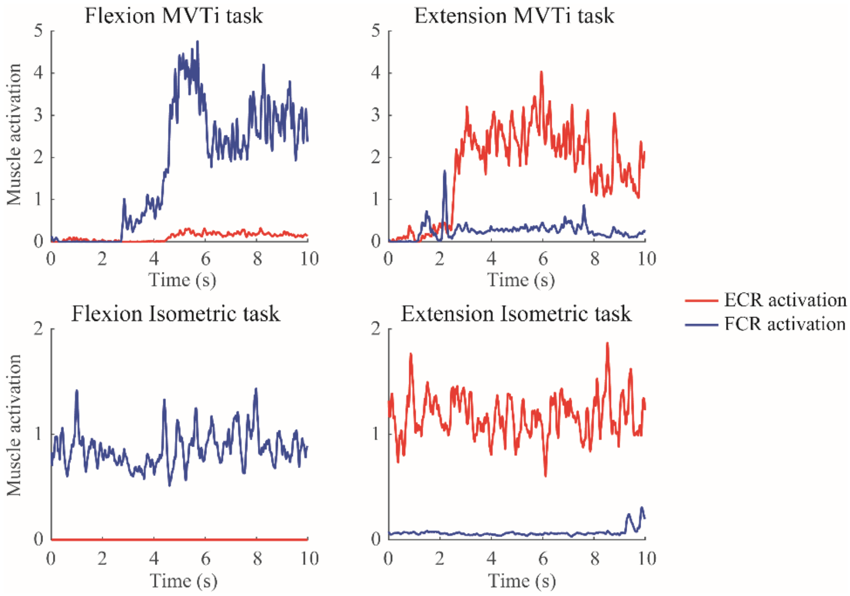

Fig. 6: Example of muscle activations recorded during two repetitions of the MVT$_i$ and isometric tasks. ECR (red lines) and FCR (blue lines) activations (Butterworth 2nd order filtered between 20 and 500 Hz, rectified, resampled at 100 Hz, baseline subtracted and normalized) recorded during a flexion (up-left panel) and an extension (up-right) MVT$_i$ tasks and during a flexion (down-left panel) and an extension (down-right) isometric tasks, performed by participant 1.

3.1. Initial maximum voluntary torques

No difference among the MVT exerted at the beginning of different sessions (see Fig. 7) was detected during both the flexion and extension tasks (ANOVA on MVT_{Ei}. p= 0.767; MVT_{Fi}, p= 0.636), thus we conclude that there was no bias in the initial fatiguing.

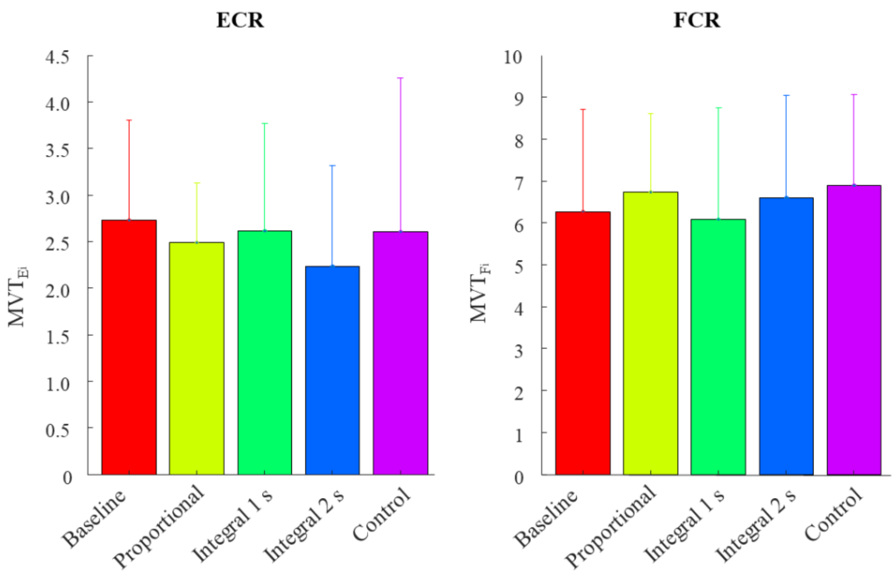

Fig. 7: Initial maximum voluntary extension torque (left), and flexion torque (right), averaged over the participants (mean ± std).

Daniele Borzelli et al 2020 J. Neural Eng. 17 016058
Doi: 10.1088/1741-2552/ab6d88
https://iopscience.iop.org/article/10.1088/1741-2552/ab6d88

3.2. Task error during tracking task

The task error was calculated during all the repetitions of the tracking task of each session, performed by each participant (see Fig. 8(A))

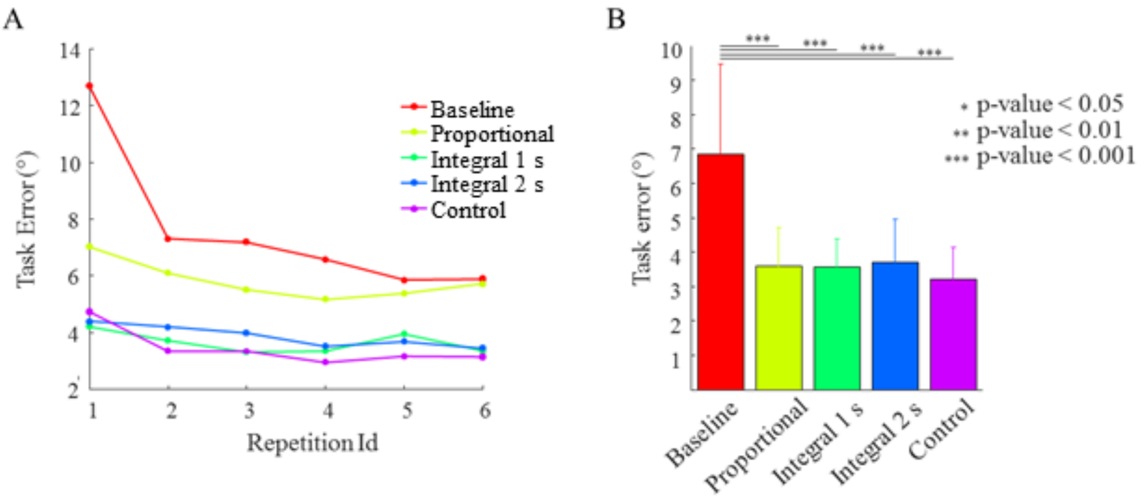

Fig. 8: Task error. (A) Examples of the task error by participant 1 during each repetition and session. (B) Mean ± std among all participants and repetitions of the task error for the different sessions.

Main effects in the differences in task error across repetitions and sessions were analyzed using a two-way ANOVA. Post-hoc test on pairs of sessions (paired t-test) identified a difference between the task error calculated during the Baseline session with respect to all the other sessions ($p < 0.001$ in all conditions). No difference in task error was identified between the Proportional session and the Integral 1s ($p > 0.854$) or Integral 2s ($p > 0.579$) sessions as well as between the Integral 1s and Integral 2s ($p > 0.338$) sessions.

Task error, averaged among participants and repetitions, was higher in the Baseline session than in all other sessions (see Fig. 8(B)). Therefore, we can conclude that if the torque perturbation is reduced by an external aid, whose action is correlated to the level of co-contraction, beneficial effects in terms of task error could be identified. However, since there was no statistical difference between the aided sessions, nothing could be said about the command strategy that guarantees minimum error.

3.3. Metabolic cost during the tracking task

The metabolic cost was calculated during all the repetitions of the tracking task of each session, performed by each participant (see Fig. 9(A)).

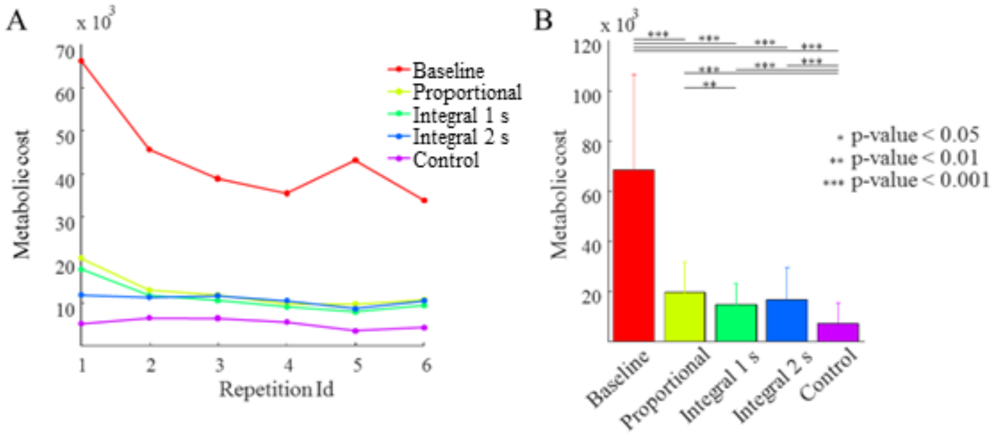

Fig. 9: Metabolic cost. (A) Examples of the energy consumption of participant 1 during each repetition and session. (B) Mean ± std among all participants and repetitions of the energy consumption for the different sessions.

Differences in metabolic cost across repetitions and sessions were tested with a two-way repeated measure ANOVA. A main effect of both sessions and repetitions was found ($p < 0.001$). A post-hoc test on pairs of sessions (paired t-test) identified a difference between the metabolic cost calculated during the baseline session with respect to all the other sessions ($p < 0.001$), between the control session and all the other sessions ($p < 0.001$), as well as between the Proportional and Integral 1s sessions ($p < 0.006$). No difference was identified between the metabolic cost calculated during the Proportional and Integral 2s sessions ($p > 0.063$) as well as between Integral 1s and Integral 2s sessions ($p > 0.309$).

Consistently with the analysis performed on the task error, the metabolic cost, averaged among participants and repetitions, calculated during the Baseline session was higher than during all other sessions (see Fig. 9(B)). Moreover, the metabolic cost calculated during the Control session was lower than during all other sessions. Among the aided sessions, the metabolic cost calculated during the Proportional session was the highest, while the metabolic cost calculated during the Integral 1s session was the lowest. Therefore, we can conclude that if the torque perturbation is reduced by an external aid, beneficial effects in terms of metabolic cost could be identified. On the other hand, the Integral 1s session led to a lower metabolic cost with respect to the Proportional session. This metabolic cost reduction was not due to a task error augmentation. However, since no statistical difference was identified between the Integral 2s session with respect to both the Proportional and the Integral 1s session, nothing could be said about the best command strategy between the proposed ones.

3.4. Median frequency

The median frequency of the EMG signal of FCR, recorded during the exertion of the isometric flexion torque, and ECR, recorded during the exertion of the isometric extension torque, was calculated during each repetition (see Fig. 10(A)). The increase of the median frequency, which is a consequence of the higher number of motor units recruited during the task, is indicative of fatigue [26]. In particular, the increase of the median frequency, indicated by the positive slope of the regression line of the median frequency as a function of task repetition number, can be used to assess muscular fatigue. The regression slope was calculated for FCR during the isometric flexion task, and for ECR during the extension task, for each participant and session. The Difference in the slopes across sessions was examined using a one-way ANOVA repeated measure.

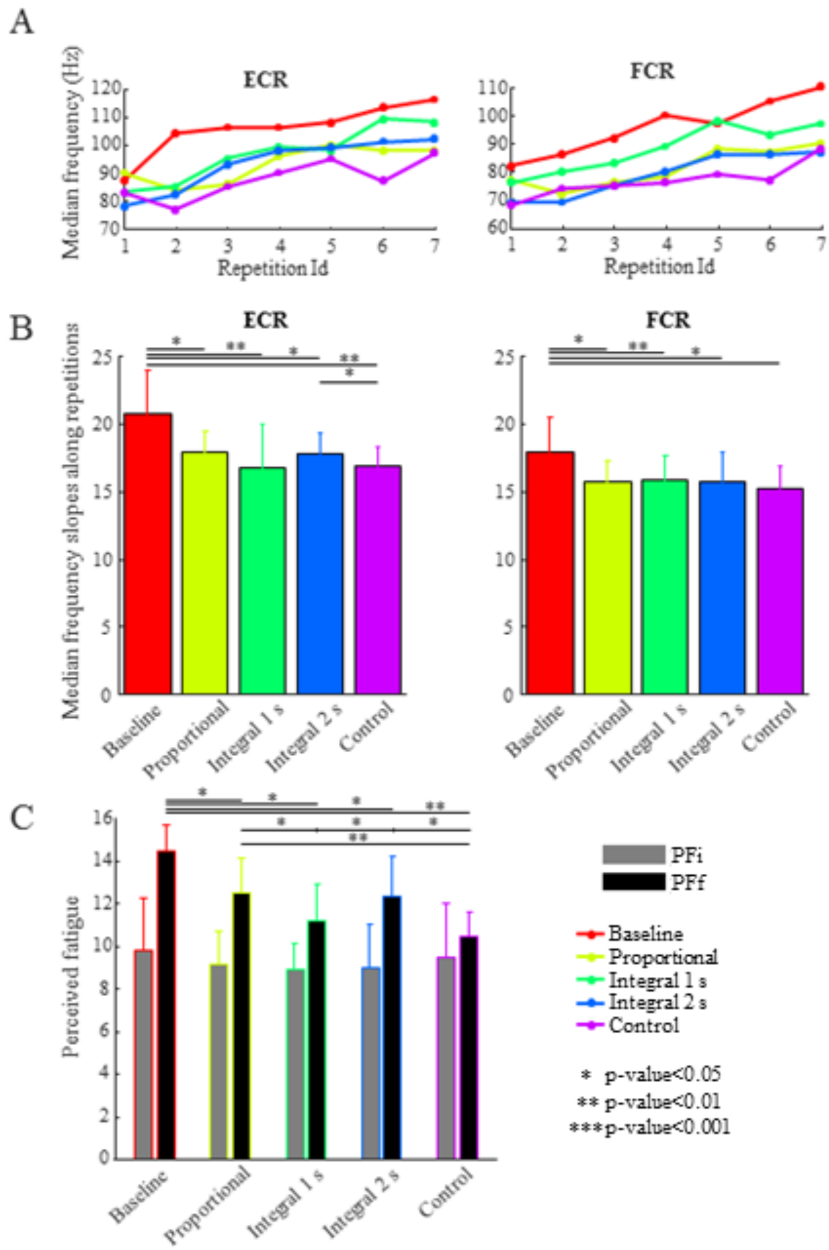

Fig. 10: Median frequency and perceived fatigue. (A) Example of the median frequency of Participant 1 in the ECR (left, calculated during all the repetitions of the extension isometric task) and FCR (right, calculated during all the repetitions of the flexion isometric task). (B) Slope of the regression of the median frequency as a function of repetition number for ECR (left) and FCR (right) in each session (mean ± std across participants). (C) Initial (grey) and final (black) perceived fatigue of each session based on the RPE CR10 Borg scale.

There was an effect of session on the ECR slopes ($p < 0.003$). Post-hoc test on pairs of sessions (paired t-test) identified a statistically significant difference between the median frequency slope recorded during the Baseline session with respect to all other sessions (p-value with respect to Proportional: 0.041, relative to Integral 1s: 0.006, Integral 2s: 0.017, Control: 0.006), and between the Integral 2s session with respect Control session ($p > 0.019$) (Figure 10(B), left). No statistical difference was identified between the slope recorded during the Proportional session with respect to the Integral 1s ($p > 0.446$) session, the Integral 2s ($p > 0.963$), and the Control ($p > 0.122$) sessions and between Integral 1s with respect to the Integral 2s ($p > 0.260$) and Control ($p > 0.903$) sessions. While an increase of the median frequency was identified along repetitions, some sessions showed a decrease of the metabolic cost along repetitions (e.g. see Baseline, Proportional, and Integral 1 s in Fig. 9(A)). This was not surprising because the metabolic cost was calculated from the amplitude of the muscle activations, while the median frequency from its frequency, two measures that are not necessarily related [29], and the discrepancy could be due to the recruitment of different pools of motor units during different repetitions (e.g. fast fatiguing motor units may be recruited during the only initial repetitions).

There was also an effect of session on the FCR slopes ($p < 0.006$). Post-hoc test on pairs of sessions (paired t-test) identified a difference between the median frequency slope recorded during the Baseline session with respect to all the other sessions (p-value with respect to Proportional: 0.025, Integral 1s: 0.027, Integral 2s: 0.022, Control: 0.031) (Figure 10(B), right). No statistical difference was identified between the slope recorded during the Proportional session with respect to the Integral 1s session ($p > 0.854$), the Integral 2s ($p > 0.952$), and the Control ($p > 0.478$) sessions, between the Integral 1s with respect to the Integral 2s ($p > 0.916$) and the Control ($p > 0.234$) sessions, and between the Integral 2s with respect to the Control ($p > 0.316$) sessions.

In sum, the higher slope of the median frequency of both ECR and FCR in the Baseline session with respect to all the other sessions (see Fig. 10(B)) indicated that higher fatigue occurred if no aid was provided.

3.5. Perceived fatigue

The fatigue perceived by the participants at the beginning of each session were compared with a Friedman test for paired samples. The same Friedman test was used to test the statistical difference between the fatigue each participant perceived at the end of each session. Consistently with the MVT_i, no effect of session was identified in the perceived fatigue at the beginning of the experiment ($p > 0.653$). Therefore, no bias in the perceived fatigue at the beginning of the session could be identified across sessions. However, there was a significant effect of session on the perceived fatigue at the end of the session ($p < 0.001$). In particular, post-hoc test on pairs of sessions (Wilcoxon signed-rank test) identified a statistically significant difference in the fatigue perceived at the end of the Baseline session with respect to all the other sessions (Wilcoxon test of difference with respect to Proportional: $p < 0.023$, Integral 1s: $p < 0.015$, Integral 2s: $p < 0.026$, Control: $p < 0.009$), between the fatigue perceived at the end of Integral 1s with respect to the Proportional ($p < 0.012$) and Integral 2s ($p < 0.019$) sessions, and between the Control session with respect to the Proportional ($p < 0.009$) and the Integral 2s ($p < 0.023$) sessions. No statistically significant difference was found between the fatigue perceived at the end of the Proportional with respect to the Integral 2s ($p > 0.824$) sessions and between Integral 1s with respect to the Control ($p > 0.081$) sessions.

The fatigue perceived at the end of the Baseline session, averaged across all participants, was higher than the fatigue perceived at the end of all the other sessions, which suggested that participants perceived the Baseline as the most fatiguing session (Fig. 10(C)). The fatigue perceived at the end of the Integral 1s session and at the end of the Control sessions were lower with respect to the fatigue perceived at the end of all the other sessions, suggesting that participants perceived the Integral 1s and the Control as the less fatiguing sessions. Since there was no difference between sessions in the initial trial, differences among the perceived fatigue at the end of the session are not due to initial biases.

4. Discussion

In this study, we experimentally compared different stiffness control strategies of an EMG-driven robotic device. Subjects performed a tracking task with their right wrist, during five experimental sessions, while a perturbative sinusoidal torque was applied by a haptic device. We demonstrated that a strategy that increased the robotic device stiffness via software, based on the previous co-contraction estimated from EMG, led to beneficial effects in terms of metabolic cost, tracking error and perceived fatigue. Lower fatigue was perceived if the torque was reduced proportionally to the mean co-contraction calculated in the previous 1 s.

Previous studies demonstrated that human subjects increase the stiffness of their limb to reject perturbations [30]–[32] or to perform tasks that require high accuracy [33], [34]. Therefore, different groups implemented a control of stiffness in their robotic devices, based on the EMG signal collected from the operator [11]–[16]. However, the stiffness modulation was achieved sample-by-sample proportionally to the stiffness estimated from the EMG signal collected from the operator.

Since operators were demonstrated to prefer working with high stiffening levels [19], a sample-by-sample strategy may lead to fatigue, which may compromise the positive effect of the robotic device and would reduce the feasible strategies the operator may exploit during the task. Therefore, we proposed to control the stiffness of a robotic device not proportionally to the co-contraction calculated at a single time sample (Proportional session), but according to the co-contraction calculated in a specific preceding time interval, in particular equal to 1 s (Integral 1s) or 2 s (Integral 2s). We investigated the effects of these three command strategies in terms of muscle fatigue, task error, metabolic cost, and perceived fatigue. The aided sessions (Proportional, Integral 1s, and Integral 2s sessions) were compared with a non-aided session (Baseline), in which no perturbation reduction was made via software, and a non-perturbed session (Control), in which participants were required only to track the target without stiffening the limb.

Beneficial effects of an external aid

Participants were able to flex and extend the wrist, to track a virtual cursor, and to increase co-contraction at the same time. These were two competing requirements because tracking required a selective activation of one muscle, with a consequent inhibition of the antagonist, and stiffening required the simultaneous recruitment of both muscles. This indicates that the CNS can modulate the muscle activations of antagonistic muscle such as to satisfy both competing tasks at the same time.

The median frequency of the EMG signal, calculated during sub-maximal isometric tasks that alternated with the tracking task during all sessions, was investigated to assess muscular fatigue [26]. Since an increase of the median frequency was observed, we concluded that both the FCR and the ECR muscles were fatiguing during all the sessions. However, a higher slope was identified during the Baseline session than in aided sessions, suggesting that all command strategies used to aid the performance of the task in presence of a perturbation succeeded in reducing fatigue. Reduced task error and reduced metabolic cost were observed during the tracking tasks performed during the aided sessions, as well as a reduced fatigue was perceived by participants at the end of aided sessions. All these results support the hypothesis that an external device, which modulates its stiffness based on the stiffness exerted by the operator, estimated from the EMG signal, leads to beneficial effects.

Preferable command strategy

A lower metabolic cost was identified during the Integral 1s and the Integral 2s sessions with respect to the Proportional session. Since this observation was not accompanied with differences in the tracking error across aided sessions, we could conclude that participants preferred a command strategy based on the mean co-contraction over a time interval rather than sample-by-sample to reduce the external perturbation. In fact, the Integral strategy allowed to exploite a larger range of muscle control strategies to be used to achieve the same performance with a lower metabolic cost. During a dynamic task, the muscles involved in the movement generate different levels of force, depending on the limb posture and joint velocities, given that muscle tension depends on the velocity of contraction and the fiber length [35]. If the Proportional strategy is implemented in a task that requires additional co-contraction, the operator would need to increase the activation of his/her muscles to achieve, at least, the minimum required for the desired performance, during the whole trial. On the contrary, an Integral control strategy allows to co-contract more only during those phases of the trial in which less effort (i.e. less muscle activity) is required. This latter strategy would then result in a reduced metabolic cost for the same trial performance. Had the participants exerted a constant co-contraction during the whole trial, which is the optimal strategy with Proportional control, they would not have been able to discern among the aided sessions. Since participants generated non-constant levels of co-contraction across the trial, associated with non-constant metabolic cost (see Fig. 5, bottom panel), the Integral control strategy permits a higher flexibility to the Central Nervous System. In contrast, a feedback based on the activity collected in the previous 2 s, as in the Integral 2 s control strategy, may be too delayed to allow the participant to identify a cause-effect relation between the voluntary co-contraction modulation and the perceived perturbation reduction.

While there was no statistically significant difference among the metabolic cost calculated during the Integral 1s and Integral 2s sessions, participants felt lower fatigue using the Integral 1s than the Integral 2s or Proportional command strategies. We thus can propose that the Integral 1s session is preferable to the other command strategies tested here.

Significance and applications

We questioned whether a Proportional strategy, largely implemented in myo-controlled robotic devices for the control of force [7], could also be an optimal solution for the control of stiffness. Since the strategy based on the mean stiffness estimated from the operator in the previous 1 s was identified to be preferable, we propose that two separate strategies could be implemented for the control of force (Proportional) and stiffness (Integral 1 s). Similarly, the Central Nervous System has been shown to independently control the muscles to move and to stiffen a limb [36].

The proposed control strategy could be implemented in any myo-controlled robotic device designed to aid the operator during dynamic tasks in which stiffening may be required, e.g. industrial, medical, or military exoskeletons, prosthesis, or myo-controlled robots. It could also be coupled with EMG-driven musculoskeletal models for the real-time estimation of the stiffness generated by the operator [37].

Limitations in the study

Similarly to previous studies, which estimated the stiffness of a participant based on the activation of only two muscles [38-44], we reduced the amplitude of the perturbation proportionally to the co-contraction of two antagonist wrist muscles. However, many more muscles act on the same joint, and recording the activity of only two muscles reduces the redundancy of the musculoskeletal system that could be exploited to control the stiffness of the robotic device. Therefore, the command strategies that we propose should benefit from a more accurate estimation of the stiffness generated by the operator, estimated from the EMG signals acquired from additional muscles acting on additional joints [14], [37], [45-47]. However, we do not expect substantial differences in the results because different subjective (perceived fatigue) and objective variables were investigated, during both an isometric task (median frequency of EMG) and a dynamic task (task error and metabolic cost). In future work, the results we obtained should be tested during other tasks performed with more joints.

If the robotic device were required to generate a rapidly changing stiffness pattern, the Integral command strategy would likely not work properly, because of the delay introduced by the integration. However, in practice, in many tasks requiring stiffness modulation a rapid change in stiffness is not necessary, and a slow modulation of stiffness is usually enough to succeed in the task. For example, the stiffness modulation that is always required at the beginning and at the end of the task can be prepared in advance and achieved gradually.

The direction of the changes in median frequency due to fatigue depends on the specific fatiguing paradigm. In fact, the effect of fatigue identified during a long-lasting high effort isometric force generation is the reduction of the median frequency of the EMG signal [29], due to the recruitment order and the changes in the characteristics of the recruited motor units. On the contrary, during low contractions (20% 30% MVC), as the active muscle fibers become fatigued, subjects incrementally increase the motor unit firing rate as a function of the elapsed time during maximal effort [48]–[51]. Therefore, since in this study subjects were asked to generate a low isometric force for only 2 s, the fatiguing mechanisms due to a long-lasting contraction may not be involved and, therefore, we could identify the effect of fatigue as the increase of the median frequency.

Finally, this study compared three command strategies that differ in the time samples exploited to calculate the co-contraction: 2 s interval (Integral 2s), 1 s interval (Integral 1s) and 1-time sample (Proportional). However, a better solution might be identified using other, possibly intermediate, integration intervals and other time samples. Therefore, the identification of the optimal time samples on which to calculate the level of co-contraction should be tested on a larger set of conditions. Moreover, the optimal time may depend on the task, on the perturbation, and on the joint from which the signal is calculated.

Conclusion

In conclusion, in this study we tested the beneficial effects, in terms of muscle fatigue, energy consumption, tracking error, and perceived fatigue, that a human operator would have during a tracking task, performed with the wrist, if s/he uses an external device that reduces external perturbations based on the operator's co-contraction of antagonist muscles. The preferred command strategy modulated the stiffness of the robotic device based on the level of co-contraction collected during the previous 1 s.

This study aimed at identifying the best command strategy for controlling a robotic device aiding an operator to increase stiffness during tasks in a perturbative environment or that requires high accuracy. Such command strategy could be implemented in different robotic devices, such as exoskeletons, prostheses, and robots, developed for different purposes, such as rehabilitation, medical, military, or industrial purposes.

Acknowledgments

This work was supported by the Italian University Ministry (PRIN grant 2015HFWRYY).

Bibliography

[1] N. Hogan, "A review of the methods of processing EMG for use as a proportional control signal," *Biomed Eng*, vol. 11, no. 3, pp. 81–86, 1976.

[2] D. Graupe, J. Salahi, and K. H. Kohn, "Multifunctional prosthesis and orthosis control via microcomputer identification of temporal pattern differences in single-site myoelectric signals," *J. Biomed. Eng.*, vol. 4, no. 1, pp. 17–22, 1982.

[3] J. Rosen, M. Brand, M. B. Fuchs, and M. Arcan, "A myosignal-based powered exoskeleton system," *IEEE Trans. Syst. Man, Cybern. - Part A Syst. Humans*, vol. 31, no. 3, pp. 210–222, May 2001.

[4] R. Ahsan and M. I. Ibrahimy, "EMG Signal Classification for Human Computer Interaction : A Review," *Eur. J. Sci. Reseacrh*, vol. 33, no. 3, pp. 480–501, 2009.

[5] J. W. Pollock, J. Brownhill, L. M. Ferreira, C. P. McDonald, J. A. Johnson, and G. J. King, "Effect of the Posterior Bundle of the Medial Collateral Ligament on Elbow Stability," *J. Hand Surg. Am.*, vol. 34, no. 1, pp. 116–123, Jan. 2009.

[6] R. A. R. C. Gopura, D. S. V. Bandara, J. M. P. Gunasekara, and T. S., "Recent Trends in EMG-Based Control Methods for Assistive Robots," in *Electrodiagnosis in New Frontiers of Clinical Research*, 2013.

[7] R. M. Singh, S. Chatterji, and A. Kumar, "A review on surface EMG based control schemes of exoskeleton robot in stroke rehabilitation," in *Proceedings - 2013 International Conference on Machine Intelligence Research and Advancement, ICMIRA 2013*, 2014, pp. 310–315.

[8] P. Maciejasz, J. Eschweiler, K. Gerlach-Hahn, A. Jansen-Troy, and S. Leonhardt, "A survey on robotic devices for upper limb rehabilitation," *Journal of NeuroEngineering and*

Rehabilitation, vol. 11, no. 1. 2014.

[9] T. Shahid, D. Gouwanda, S. G. Nurzaman, and A. A. Gopalai, “Moving toward Soft Robotics: A Decade Review of the Design of Hand Exoskeletons,” *Biomimetics*, vol. 3, no. 3, p. 17, 2018.

[10] N. Hogan, “Impedance control: An approach to manipulation,” *Am. Control Conf. 1984*, 1984.

[11] C. J. Abul-Haj and N. Hogan, “Functional assessment of control systems for cybernetic elbow prostheses (2 Parts).,” *IEEE Trans. Biomed. Eng.*, vol. 37, no. 11, pp. 1037–47, 1990.

[12] T. Tsuj, O. Fukuda, H. Shigeyoshi, and M. Kaneko, “Bio-mimetic impedance control of an EMG-controlled prosthetic hand,” in *Proceedings of the 2000 IEEE/RSJ International Conference on Intelligent Robots and Systems*, 2002, pp. 377–382.

[13] S. Lee and Y. Sankai, “Power assist control for walking aid with HAL-3 based on EMG and impedance adjustment around knee joint,” in *IEEE/RSJ International Conference on Intelligent Robots and System*, 2002, vol. 2, pp. 1499–1504.

[14] A. Ajoudani, N. Tsagarakis, and A. Bicchi, “Tele-impedance: Teleoperation with impedance regulation using a body-machine interface,” *Int. J. Rob. Res.*, vol. 0, no. 0, pp. 1–14, 2012.

[15] P. Liang, C. Yang, N. Wang, and Z. Li, “Implementation and Test of Human-Operated and Human-Like Adaptive Impedance Controls on Baxter Robot,” *Adv. Auton. …*, 2014.

[16] Z. Li, Z. Huang, W. He, and C. Y. Su, “Adaptive impedance control for an upper limb robotic exoskeleton using biological signals,” *IEEE Trans. Ind. Electron.*, vol. 64, no. 2, pp. 1664–1674, 2017.

[17] S. Yao, Y. Zhuang, Z. Li, and R. Song, “Adaptive admittance control for an ankle exoskeleton using an EMG-driven musculoskeletal model,” *Front. Neurorobot.*, vol. 12, no. APR, 2018.

[18] W. Gallagher, D. Gao, and J. Ueda, “Improved stability of haptic human-robot interfaces using measurement of human arm stiffness,” *Adv. Robot.*, vol. 28, no. 13, pp. 869–882, 2014.

[19] J. W. Sensinger and R. F. F. Weir, “User-modulated impedance control of a prosthetic elbow in unconstrained, perturbed motion,” *IEEE Trans. Biomed. Eng.*, vol. 55, no. 3, pp. 1043–1055, 2008.

[20] A. Melendez-Calderon, L. Bagutti, B. Pedrono, and E. Burdet, “Hi5: A versatile dual-wrist device to study human-human interaction and bimanual control,” in *2011 IEEE/RSJ International Conference on Intelligent Robots and Systems*, 2011, pp. 2578–2583.

[21] A. Melendez-Calderon, V. Komisar, and E. Burdet, “Interpersonal strategies for disturbance attenuation during a rhythmic joint motor action,” *Physiol. Behav.*, vol. 147, pp. 348–358, 2015.

[22] H. Hermens, B. Freriks, R. Merletti, G. Hägg, D. Stegeman, J. Blok, G. Rau, and C. Disselhorst-Klug, *European Recommendations for Surface ElectroMyoGraphy, deliverable of the SENIAM project*. 1999.

[23] F. Kendall, E. McCreary, and P. Provance, “Muscles, Testing and Function,” *Med. Sci. Sports Exerc.*, vol. 26, no. 8, p. 1070, 1994.

[24] T. Zachry, G. Wulf, J. Mercer, and N. Bezodis, "Increased movement accuracy and reduced EMG activity as the result of adopting an external focus of attention," *Brain Res. Bull.*, vol. 67, no. 4, pp. 304–309, 2005.

[25] G. Borg, "Borg's perceived exertion and pain scales," *Hum. Kinet.*, 1998.

[26] R. Merletti and P. A. Parker, *Electromyography : physiology, engineering, and noninvasive applications*. IEEE Press, 2004.

[27] M. a Mañanas, R. Jané, J. a Fiz, J. Morera, and P. Caminal, "Influence of estimators of spectral density on the analysis of electromyographic and vibromyographic signals.," *Med. Biol. Eng. Comput.*, vol. 40, no. 1, pp. 90–8, 2002.

[28] M. González-Izal, A. Malanda, E. Gorostiaga, and M. Izquierdo, "Electromyographic models to assess muscle fatigue," *Journal of Electromyography and Kinesiology*, vol. 22, no. 4. pp. 501–512, 2012.

[29] N. A. Kamaruddin, P. I. Khalid, and A. Z. Shaameri, "The use of surface electromyography in muscle fatigue assessments–a review," *J. Teknol.*, vol. 74, no. 6, pp. 119–124, 2015.

[30] T. Milner, "Adaptation to destabilizing dynamics by means of muscle cocontraction," *Exp. Brain Res.*, 2002.

[31] E. Burdet, R. Osu, D. Franklin, T. Milner, and M. Kawato, "The central nervous system stabilizes unstable dynamics by learning optimal impedance," *Nature*, vol. 414, pp. 446–449, 2001.

[32] S. J. De Serres and T. E. Milner, "Wrist muscle activation patterns and stiffness associated with stable and unstable mechanical loads," *Exp. Brain Res.*, vol. 86, no. 2, pp. 451–458, 1991.

[33] L. P. J. Selen, D. W. Franklin, and D. M. Wolpert, "Impedance control reduces instability that arises from motor noise," *J. Neurosci.*, vol. 29, no. 40, pp. 12606–12616, Oct. 2009.

[34] P. L. Gribble, L. I. Mullin, N. Cothros, and A. Mattar, "Role of cocontraction in arm movement accuracy," *J. Neurophysiol.*, vol. 89, no. 5, pp. 2396–2405, May 2003.

[35] H. Hatze, "A myocybernetic model of skeletal muscle," *Biol. Cybern.*, vol. 28, pp. 143–157, 1978.

[36] D. R. Reed and D. R. Humphrey, "A model of motor unit recruitment which results in independent control of equilibrium position and stiffness of the joint," *Soc. Neurosci. Abstr.*, vol. 17, 1991.

[37] G. Durandau, D. Farina, and M. Sartori, "Robust Real-Time Musculoskeletal Modeling Driven by Electromyograms," *IEEE Trans. Biomed. Eng.*, vol. 65, no. 3, pp. 556–564, 2018.

[38] E. Hocaoglu and V. Patoglu, "Tele-impedance control of a variable stiffness prosthetic hand," 2012, pp. 1576–1582.

[39] N. Karavas, A. Ajoudani, N. Tsagarakis, J. Saglia, A. Bicchi, and D. Caldwell, "Tele-impedance based assistive control for a compliant knee exoskeleton," in *Robotics and Autonomous Systems*, 2015, vol. 73, pp. 78–90.

[40] S. Mghames, M. Laghi, C. Della Santina, M. Garabini, M. Catalano, G. Grioli, and A. Bicchi, "Design, control and validation of the variable stiffness exoskeleton FLExo," in *2017 International Conference on Rehabilitation Robotics (ICORR)*, 2017, pp. 539–546.

[41] B. J. E. Misgeld, T. Zhang, M. J. Lüken, and S. Leonhardt, "Model-based estimation of ankle joint stiffness," *Sensors (Switzerland)*, vol. 17, no. 4, p. 713, 2017.

[42] D. Borzelli, S. Pastorelli, and L. Gastaldi, "Model of the human arm stiffness exerted by two antagonist muscles," in *Advances in Intelligent Systems and Computing*, 2017, vol. 540.

[43] D. Borzelli, S. Pastorelli, and L. Gastaldi, "Elbow musculoskeletal model for industrial exoskeleton with modulated impedance based on operator's arm stiffness," *Int. J. Autom. Technol.*, vol. 11, no. 3, 2017.

[44] D. Borzelli, S. Pastorelli, and L. Gastaldi, "Determination of the human arm stiffness efficiency with a two antagonist muscles model," in *Mechanisms and Machine Science*, 2017, vol. 47.

[45] E. Burdet, D. W. Franklin, and T. E. Milner, *Human robotics*. MIT Press, 2013.

[46] P. Liang, C. Yang, N. Wang, and R. Li, "A Discrete-Time Algorithm for Stiffness Extraction from sEMG and Its Application in Antidisturbance Teleoperation," *Discret. Dyn. Nat. Soc.*, vol. 2016, 2016.

[47] D. Borzelli, B. Cesqui, D. J. Berger, E. Burdet, and A. D'Avella, "Muscle patterns underlying voluntary modulation of co-contraction," *PLoS One*, vol. 13, no. 10, p. e0205911, 2018.

[48] D. Gamet and B. Maton, "The fatigability of two agonistic muscles in human isometric voluntary submaximal contraction: an EMG study," *Eur. J. Appl. Physiol. Occup. Physiol.*, vol. 58, no. 4, pp. 361–368, 1989.

[49] L. J. Dorfman, J. E. Howard, and K. C. McGill, "Triphasic behavioral response of motor units to submaximal fatiguing exercise," *Muscle Nerve*, vol. 13, no. 7, pp. 621–628, 1990.

[50] A. Adam and C. J. De Luca, "Firing rates of motor units in human vastus lateralis muscle during fatiguing isometric contractions," *J. Appl. Physiol.*, vol. 99, no. 1, pp. 268–280, 2005.

[51] J. L. Taylor and S. C. Gandevia, "A comparison of central aspects of fatigue in submaximal and maximal voluntary contractions," *Journal of Applied Physiology*, vol. 104, no. 2. pp. 542–550, 2008.